Author Comment to Referee #1

ACP Discussions doi: 10.5194/acp-2018-724
(Editor - Peter Haynes)
'Lagrangian simulations of the transport of young air masses to the top of the Asian monsoon anticyclone and into the tropical pipe'

We thank Referee #1 for further guidance on how to to revise our paper. Following the reviewers advice we revised some parts of the paper for the purpose of clarification. In particular, we want to thank the reviewer for the elaborate language corrections. This was a very great support. Our reply to the reviewer comments is listed in detail below. Questions and comments of the referee are shown in italics. Passages from the revised version of the manuscript are shown in blue.

This manuscript uses back trajectories and full 3D CLaMS simulations in conjunction with MIPAS HCFC-22 measurements to elucidate the transport pathway of air masses emitted in defined boundary layer regions through the Asian summer monsoon anticyclone and into the tropical pipe. The modeling tools and measurements are well suited to the investigation, the analysis is generally well thought out and well executed, and the findings will certainly be of interest to the journal readership. I do, however, have a number of substantive comments that I would like to see addressed before the paper is accepted for publication in ACP.

Specific substantive comments and questions:

Sections 2.2 and 3.2.1: 40 days seems like a very long period for trajectory calculations. I realize that CLaMS 40-day trajectories have been published previously, but nevertheless I think that a sentence or two on how much error has accumulated over the course of such long trajectory calculations would be appropriate, either in Section 2.2 or in Section 3.2.1.

We agree and have thus added a few sentences in Section 3.2.1. to discuss the errors of the trajectory length as follows.

In general, trajectory calculations have limitations due to trajectory dispersion by errors through interpolation of the wind data to the position of the air parcel at a specific time. Over the timescales in question, mixing can also be relevant (e.g., McKenna et al., 2002). These errors can accumulate depending on the trajectory length over the course of the simulation. However, the frequently employed trajectory length to study transport processes in the Asian monsoon region is ranging from a couple of weeks to a few months (e.g., Chen et al., 2012; Bergman et al., 2013; Vogel et al., 2014; Garny and Randel, 2016; Müller et al., 2016; Li et al., 2017). In our trajectory analysis, the focus is to demonstrate the large-scale transport pathways of the air parcels at the top of the anticyclone, small changes of the trajectory position will therefore not affect our findings.

Section 2.4: I miss in the description of the MIPAS HCFC-22 any information about the accuracy, precision, or horizontal or vertical resolution of the measurements. Some discussion of the data quality is warranted to help evaluate the comparisons with CLaMS results later in the manuscript. This information may be contained in the paper by Chirkov et al., but some basic data quality information needs to be included here as well for the convenience of the reader. See related comment below.

As suggested we provide some additional information about the MIPAS HCFC-22 data quality in Section 2.4 as follows.

The limited vertical resolution of the MIPAS HCFC-22 data needs to be taken into account in comparisons to model results. The precision of an individual data point in the altitude region of the Asian monsoon tropopause is 7 to 8 pptv in terms of measurement noise. Parameter errors contribute to a total uncertainty of about 15 pptv in this region for each data point. Thus, the scatter of the HCFC-22 data points (e.g. as shown in Fig. 3) is consistent to the total error. According to Chirkov et al. (2016), the vertical resolution (in terms of the full width at half maximum of the vertical averaging kernel) increases from about 3.3 km at 12 km to 5.5 km at 20 km altitude (see Fig. 2 in Chirkov et al., 2016).The horizontal resolution (in terms of the full width at half maximum of the horizontal averaging kernel) increases from 300 km at 15 km altitude to 600 km at 20 km altitude. Given the rather smooth profiles expected in this study, the limited altitude resolution has a minor effect only; in contrast, it turns out to be crucial when highly structured profiles, such as typically occur at the edge of the polar vortex, are analysed. Further it has to be noted that tropical HCFC-22 profiles from MIPAS seem to have a high bias below 30 km, that, however, is broadly constant with altitude (Chirkov et al., 2016); thus, it does not affect the comparisons made here.

P7, L29 - P8, L11: These paragraphs are confusing, because the first sentence (P7, L29), as well as the subsection title, refer to transport of emission tracers to 'the top of the Asian monsoon anticyclone', yet Figure 2 (top row) and the related discussion focus on 360 K, which is obviously not at the top of the anticyclone. It may be that the discussion begins with 360 K because that level is where regions 'inside' and 'outside' the anticyclone are defined, which seems to be what is implied by the sentence in P8, L9-10, but if so then that motivation needs to come earlier in the paragraph to set the stage. Moreover, if that is the case, then I am confused by that as well - why define inside/outside the anticyclone at a single level, rather than at each considered level, since the shape of the anticyclone changes considerably with height? And Fig. 3 defines the anticyclone by the 20% contour of the India/China tracer at 380 K (not 360 K). So this entire discussion needs to be clarified.

We agree that here we have to provide a better motivation to explain our analysis. We introduced a motivation/introduction to Sect. 3.1.1 as follows.

It is known that the Asian monsoon anticyclone has a strong horizontal transport barrier at about 380 K (e.g., Ploeger et al., 2015), however this transport barrier is not well defined at higher levels of potential temperature. The less strong transport barrier at higher levels has consequences on the vertical transport at the top of the anticyclone. Before the transport at the top is discussed we show the horizontal distribution of different emission tracers at 360 K and then their subsequent transport to the top of the anticyclone up to 460 K. Vogel et al. (2015) showed that the emission tracer for India/China is a good proxy for the location and shape of the Asian monsoon anticyclone using pattern correlations with potential vorticity (PV), and MLS O_3 and CO satellite measurements between 360 K and 400 K. Therefore here we use the India/China tracer as proxy for the location of the anticyclone.

P8, L15: To my eye, it looks as though fractions as high as 40% extend lower than 350 K, down to at least 340 K, if not lower.

Yes, we agree the fractions as high as 40% extend lower down to ≈340 K. We revised the paragraph as follows.

We would like to emphasise the horizontal transport of air masses with high contributions from India/China (40%–90%) from the eastern part of the anticyclone to both the western part and into the eddy over the western Pacific between ≈340 K and ≈380 K.

P8, L20-21: It is not clear exactly which regions are being referred to for these values; in particular, in some areas (≈310-330 K, 10N) fractions from the tropical adjacent regions much higher than 10%-40% are seen.

We revised this paragraph to be more precise as follows.

In the western mode there is still a high contribution from the India/China tracer between 20% and 60% and lower fractions about 10%–40% from the tropical adjacent regions (Fig. 2g/h inside the thick white line). Below the western mode, in the tropics below ≈330 K at around 10°N fractions from the tropical adjacent regions (in that case from Northern Africa) are up to 90% caused by local upward transport.

P8, L28-29: First, the region 'inside the anticyclone' is referred to here, but it is not possible for the reader to identify where the anticyclone boundary falls at different altitudes in the cross sections of Fig. 2. The authors should think about how to convey information about the approximate location of the anticyclone in these panels. Second, it is stated that near the tropopause the fraction from the tropical adjacent regions reaches as high as 35%, but I am not sure exactly where is being referred to, as most TAR fractions in the vicinity of the monsoon in Fig. 2d are no larger than 25-30%.

A clear definition of the edge anticyclone over a large range of different altitudes is not possible such as a PV-based criterion (e.g., Ploeger et al., 2015). We use here as a proxy the distribution of the India/China tracer. Further, we agree the TAR fractions are to about 30%. We revised the respective sentence as follows.

Below 360 K in the region with high values of the India/China tracer, the fractions from the tropical adjacent regions are below 10%, however above 360 K around the tropopause the fractions are much higher, up to about 30%, and up to about 15% around 420 K (see Fig. 2d/f).

P9, L11-25: I agree that the HCFC-22 data show good agreement with the India/China emission tracer and that they are a very useful element of the analysis. However, Fig. 3 reveals quite a few stray data points well outside the anticyclone that also have elevated HCFC-22 abundances. As mentioned earlier, the precision of an individual data point should be given so that the agreement in Fig. 3 can be fully evaluated. It seems to me that the enhancement in the thin filament (L15) does not particularly stand out in the measurements; indeed, in the absence of the CLaMS results to guide the eye, it likely would be overlooked altogether. Likewise, the measured enhancements at the top of the anticyclone above the tropopause (L20) are also fairly modest; in fact, they are not much different from other high MIPAS points well away from where CLaMS indicates a signal (e.g., at the EQ at 370 K, at 5N at 420 K, and at 30N at 430 K). It might help to also overlay on these plots (both the map and the cross sections) a solid contour highlighting a selected HCFC-22 mixing ratio. Although the 'dot plots' are very valuable for representing the sampling of the MIPAS measurements, they do make it more difficult to get an impression of the overall morphology. Overlaying one specific contour from a gridded HCFC-22 field might strengthen the case for good agreement with the modeled tracer. Finally, although I do see a steep vertical gradient in the HCFC-22 data from ≈350 to 360 K in the ≈25-40N region, I do not see a corresponding signature in the India/China tracer in that region (L25); there is a steep gradient in that tracer in Fig. 2g, but at altitudes below 350 K, so the patterns in the 350-360 K region are not really that similar.

We thank the reviewer for the advice to modify Fig. 3 by overlaying a solid contour highlighting a selected HCFC-22 mixing ratio. We tested different plotting types as shown in Fig. 1 of this author comment. Because of the coarse vertical resolution of the MIPAS measurements a solid contour depends strongly on the grid used for interpolation. Therefore, we prefer to show the plots without a solid contour line for a selected HCFC-22 mixing ratio.

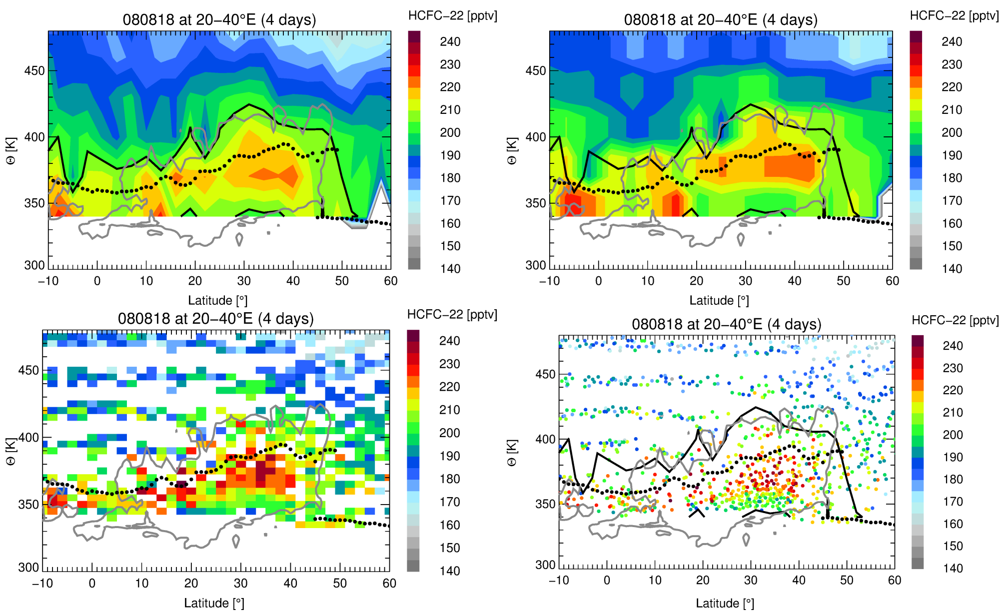

Figure 1: Latitude–theta cross sections at 30°E (western part of the anticyclone) on 18 August 2008: contour plot, contour plot with a resampled finer grid (congrid), plotcell, and xy-plot. The contour line of 200 pptv HCFC-22 is shown in black. The contour line of 20% of the India/China tracer is shown by thick grey lines.

P10, L6-11: Again, this discussion refers to 'within' and 'in the core of' the anticyclone, so some means of delineating exactly where that region is at each level is needed. In Fig. 3, the 20% contour for the India/China tracer is used to approximate the boundary of the anticyclone at 380 K, but what about at the higher levels shown in Fig. 4? How is the reader to gauge that the largest contributions of both emission tracers are found within the anticyclone at 400 K but around its edge at 420-460 K, as stated here? In fact, I am not convinced that either statement is true: the eastern lobe of the anticyclone (≈100E) shows the largest fractions of the TAR tracer along what looks to me more like the edge of the anticyclone at 400 K, whereas the largest values of both tracers seem to be concentrated in the core region at that longitude at 420 K.

We agree that this discussion is a bit confusing. We revised this paragraph as follows.

Young air masses (age $<$ 6 months) from both India/China and tropical adjacent regions are found up to $\approx$460 K. It was shown earlier that the horizontal distribution of the India/China tracer is a good proxy for the location of the anticyclone (Vogel et al., 2015). The horizontal distribution of the tropical adjacent regions compared to the horizontal distribution of the India/China tracer strongly differs depending on the level of potential temperature from a nearly disjoint distribution at 360 K (see Fig. 2) to a more coincident distribution from 400 K to 460 K (see Fig. 5).

At 380 K, the highest fractions from tropical adjacent regions are found at the edge of the anticyclone and at 400 K within the anticyclone. Above 400 K both tracers India/China and tropical adjacent regions show a similar horizontal distribution. We emphasise that at these levels of potential temperature the tracer distributions have the shape of rotating filaments in contrast to the more compact distribution at lower levels. The variation of the distribution of the tracer for the tropical adjacent regions with altitude is an indication that the upward transport of young air masses at the top of the anticyclone occurred more towards the edge and less inside the anticyclone itself.

P10, L16-19: How were the percentages of young air masses for the selected air parcels chosen? In the absence of any explanation these values seem arbitrary. Are these trajectories initiated from the entire region within the defined lat/lon boxes? I'm wondering if these percentages can be related to the values shown for the India/China tracer in Fig. 4.

We agree that the description of the initialisation procedure of the trajectories is a bit short. We revised this paragraph as follows.

To analyse the transport pathways to the top of the anticyclone in more detail, 40-day backward trajectories are calculated starting in the western (20–50°N,0–70°E) and eastern (20–50°N,70–140°E) modes of the anticyclone. The trajectories are started at the position of the air parcels from the 3-dimensional CLaMS simulation at different levels of potential temperature ($\Theta = 380, 400, 420, 440\,\mathrm{K} \pm 0.25\,\mathrm{K}$) on 18 August 2018. Note that the air parcels in the 3-dimensional CLaMS simulation are distributed on an irregular grid. To take into account the distribution of the boundary emission tracer at the top of the Asian monsoon anticyclone, only air parcels are selected with contributions of young air masses (age $<$ 6 months, Summer 08) larger than 70% (380 K), 50% (400 K), 20% (420 K), and 5% (440 K) (not all levels of potential temperature are presented here). The percentages are chosen in a way to obtain a number of trajectories (less than 30) that can be reasonably visualised. The results of the 40-day backward trajectories are similar at different levels of potential temperature; therefore we show a selection of trajectories to demonstrate the main transport pathway to the top of the Asian monsoon. A larger set of 20-day backward trajectories analysed statistically will be discussed below in Section 3.2.2.

P10, L22-23: How consistent are the trajectory results, which indicate that the Tibetan Plateau and the western Pacific are preferred regions for fast uplift, with prior studies (in other words, some citations would be appropriate here).

We revised this paragraph in Sect. 3.2.1 as follows and added a small discussion within Sect. 4 about convective source regions contributing to the composition of the Asian monsoon anticyclone following the advice by reviewer #2.

Fig. 5 shows trajectories started in the eastern and western part of the Asian monsoon anticyclone around the thermal tropopause at 380 K on 18 August 2018. Air masses are uplifted to approximately 360 K very rapidly by various convective events occurring at different times and locations. Our 40-day backward trajectories show that preferred regions for fast uplift are continental Asia (mainly the region of the south slope of the Himalayas and the Tibetan Plateau) and the western Pacific (not shown here). A lower fraction of trajectories originates in the free troposphere. The trajectories in Fig. 2 demonstrating convection below 380 K are only a snapshot for 18 August 2018. There are several previous studies (e.g., Randel and Park, 2006; Park et al., 2007, 2009; Wright et al., 2011; Chen et al., 2012; Bergman et al., 2013; Fadnavis et al., 2014; Tissier and Legras, 2016) quantifying the contribution of different source regions to the composition of the Asian monsoon anticyclone during the course of the monsoon season (see discussion in Sect. 4).

We added in the Discussion Section (Sect. 4) the following discussion.

It is well known that the composition of the Asian monsoon anticyclone is strongly affected by convection over continental Asia (e.g. the south slope of the Himalayas and the Tibetan Plateau), Bay of Bengal, and the western Pacific, (e.g., Randel and Park, 2006; Park et al., 2007, 2009; Wright et al., 2011; Chen et al., 2012; Bergman et al., 2013; Fadnavis et al., 2014; Tissier and Legras, 2016). However there is a debate about the contribution of different source regions to the composition of the Asian monsoon anticyclone. Further, there are differences in the conclusions in the literature about the contribution of different source regions depending on the used reanalysis data (e.g., Wright et al., 2011; Bergman et al., 2013). Findings by Vogel et al. (2015) show that there is a strong intraseasonal variability of boundary source regions to the composition of the Asian monsoon anticyclone during a particular monsoon season. We would like to emphasise that the trajectories presented in Fig. 6 demonstrating convection below 380 K are only a snapshot for 18 August 2018 with convection over the western Pacific and continental Asia mainly in the region of the south slope of the Himalayas and the Tibetan Plateau.

P10, L24-26: Is there a reason that the corresponding plots for the eastern lobe of the anticyclone were not shown in Fig. 5, as they were in Fig. 6? I would have thought that they would be relevant to the discussion here.

We didn't show the eastern mode of the anticyclone because the trajectories show similar results as for the western mode. We did not want to extend the paper to much. However, we decided to show also the plots for the eastern mode as shown in Fig. 2 (of this author comment) and Fig. 5 in the revised version of the manuscript to avoid the reader is confused why we didn't show the plots for the eastern mode.

P11, L14-26: What exactly is meant by 'substantial' upward transport (L14)? Does 'substantial' mean 0.5 K/day, 1 K/day, or?? It would be better to be more quantitative. In addition, here the discussion is cast in terms of heating rate (K per day), whereas Fig. 7 and Fig. A1 show the change in potential temperature (in K) along 20-day trajectories, making the reader do the (admittedly easy) math. Once the meaning of 'substantial' is established, it would be better to qualify the transport experienced by air parcels grouped in *filaments as being 'substantial' or 'strong' (L16) - filamentary structure is not present everywhere that air parcels have experienced some uplift. I also think it would be better to say 'largely', rather than 'only', in L26 because there are red dots outside the monsoon region, especially in July and August.*

As proposed we revised this paragraph as following including also comments by reviewer #2.

Above 360 K, air parcels that experienced strong upward transport larger than 20–30 K within 20 day (corresponding to a mean value of 1–1.5 K per day) are largely found in the region of the anticyclone. This rate of upwelling is much slower compared to convective upwelling shown at 360 K. Air parcels that experienced strong upward transport are mainly grouped in curved elongated filaments, reflecting a rotating movement of the air parcels at the top of the anticyclone. Often air parcels with strong $\Delta\Theta$ above 360 K are located more at the edge of the eastern and western modes of the anticyclone and at the edge of the eastward-migrating eddy at the eastern flank of the anticyclone. Thus the upward transport in the region of the anticyclone is inhomogeneous and not homogeneously distributed over the entire anticyclone as suggested from climatolgical studies (e.g., Randel et al., 2010; Ploeger et al., 2017). This is consistent with results presented above in Sect. 3.2.1 demonstrating that for single selected trajectories the transport at the top of the Asian monsoon anticyclone is a slow upward transport of about 1–1.5 K per day in a large-scale spiral above the anticyclone caused by diabatic heating. In the backward trajectory calculations mixing processes are not included, however the results of the trajectory calculations are consistent with patterns found in the 3-dimensional CLaMS simulation including mixing as discussed in Sect. 3.1.3, demonstrating that young air masses above 400 K are found at the edge of the anticyclone. Above 400 K, air masses in the tropics also experienced upward transport, but the vertical uplift is in general lower than 20 K within 20 day, (i.e. lower than 1 K per day).

P12, L11: It might be good to explain why the emphasis has shifted from the tropical adjacent regions examined in previous figures to Southeast Asia specifically in Fig. 9, especially since Fig. 12 shows that the TPO also makes a substantial contribution to the air at 550 K.

Many thanks for this comment. We agree that it would be more stringent to show the emission tracer for the tropical adjacent regions instead of the emission tracer for Southeast Asia in Figure 9 of the manuscript. You are right also TPO contribute much to the signal within the tropical pipe (see Fig 3 of this author comment). We changed Figure 9 in the revised version of the manuscript as shown in Fig. 4 within this author comment.

P12, L14-17: It is stated that an enhanced signal from Southeast Asia of up to 25% (L14 and L17) is seen around 550 K for the S07 pulse, but as far as I can tell from Fig. 9, the largest S07 enhancement (at ≈10S) is only ≈12%, not 25%.

Yes, we agree. However, we changed Fig. 9 (of the manuscript) showing TAR instead of SEA. For TAR 25% is correct. We changed this sentence as follows.

For the Summer 07 pulse, an enhanced signal from TAR (up to 25%) is found at around 550 K within the tropics similar as for India/China tracer.

P12, L27-28: I do think it is important to point out the uncertainties in the reanalysis heating rates, as done in these lines. However, the way this paragraph ends leaves the reader hanging a bit. What is the take-away message? Can we trust the results in Fig. 10 or not? What are the possible implications for the 'upward spiraling range'?

We revised the paragraph following the reviewers advice.

...It is known that the radiative heating rates in the tropical UTLS are different in current reanalysis models (e.g., Wright and Fueglistaler, 2013) and are most likely overestimated in ERA-Interim (e.g., Ploeger et al., 2012; Schoeberl et al., 2012). Therefore, the rates of diabatic heating in the upward spiralling range found in our study are most likely somewhat too high, however slow upward transport in the UTLS in the region of the Asian monsoon anticyclone associated with positive heating has been addressed previously (e.g., Park et al., 2007; Bergman et al., 2012; Garny and Randel, 2016; Ploeger et al., 2017).

P12, L29: It is stated that Fig. 11 shows the same cross sections as Figs. 8 and 9. The latter two figures, however, show results only for the eastern lobe (90E), whereas Fig. 11 also shows the cross section for 30E. Although we *have some information about S08 in that region from Fig. 2, we do not get the full picture from that figure, and thus we have little to compare to the left panel of Fig. 11. I note that, in terms of major features, the HCFC-22 results look quite similar at 30E and 90E. Is that also the case for the CLaMS results, that is, do the corresponding plots at 30E look similar to those in Figs. 8 and 9? If so, then that should be mentioned, and perhaps the left panel of Fig. 11 should also be omitted. If not, discussion of the differences should be included.*

Yes, we agree that the eastern mode is not shown in Figs. 8 and 9. Similar features are found in the western and eastern mode, therefore there is no added values to show the eastern mode. Following the reviewers advice the removed the plots for the eastern part.

P16, L3-4: Has evidence for a coherent signature of the existence of the anticyclone and influence of monsoon air up to altitudes as high as 460 K been reported previously? It seems to me that this may be an important finding that has been underemphasized in this manuscript.

There are a few studies looking also in this altitude range (e.g., Garny and Randel, 2016; Ploeger et al., 2017), however with an other focus. We added the following paragraph to the Discussion Sect. 4.

In this study, we focus on transport at the top of the anticyclone in an altitude range higher than 380 K potential temperature (≈100 hPa) up to 460 K (≈60 hPa). Further, in addition to previous studies (e.g., Garny and Randel, 2016; Ploeger et al., 2017), we relate the transport of air masses from inside the Asian monsoon anticyclone to air masses uplifted outside the anticyclone. Subsequently these air masses are jointly transported upwards to the top of the anticyclone at ≈460 K.

P26, Fig. 2: Perhaps it would make the maps in the top row too cluttered, but I think it would be helpful to draw on them a horizontal line at 25N and vertical lines at 30E and 90E to orient the reader for the cross sections in the bottom panels. In addition, I understand that a common color bar is used for all panels in this figure, and I agree that that is probably the best approach, and I further agree that extending the color bar to 100% is appropriate for the cross sections. However, I note that employing such a color bar renders some of the features in the maps less prominent. For example, the filament at 50E *seen so clearly at 380 K in Fig. 3, where the tracer color bar extends only to 50%, is nearly invisible in Fig. 2 but might show up well if the color bar range were reduced. I am not suggesting that the color bar should necessarily be changed, merely pointing out the issue.*

We also discussed extensively these issues. To draw three lines in Fig. 2a and 2b would make the plots very cluttered and cover some features. The color bar is a compromise between covering the full date range within the longitude-theta and latitude-theta cross sections and having the same range within the horizontal distribution at 360 K. Therefore, some features within the horizontal distribution at 360 K are less prominent. We added the following paragraph to Sect. 3.1.1.

Note that in Fig. 2 the same data range is used for all colour bars for a better comparability between the horizontal and different vertical cross sections. Therefore some features at the horizontal cross section at 360 K are not too prominent for example the thin filament at around 50°E between 40°N and 60°N in Fig. 2a (see next section Fig. 3).

P27, Fig. 3: I found the figure layout and accompanying discussion hard to follow. Here the latitude-theta cross section at 30E comes first, then the one at 90E, and finally the longitude-theta cross section, which is essentially opposite to the order followed in Fig. 2. It would make it easier to compare the CLaMS and MIPAS results if Fig. 3 were configured as a single-column figure following the same layout as Fig. 2 (with an extra panel at the top for the India/China tracer and the MIPAS panels corresponding to those in Fig. 2 below). In addition, I do not understand why only in Fig. 2 are the panels labelled. Panel labels would be helpful in Fig. 3 and all other multi-panel figures as well. This would simplify referencing the figures in the text, eliminating the need to always point to top, middle, bottom, left, right, etc.

We rearranged Fig. 3 following the reviewer's advise as shown in Figs. 5 and 6 of this author comment.

P31, Fig. 7: Again, I think this figure would work better laid out in a single column. In addition, I find the transition between upwelling and downwelling in these maps awkward - the zero value of delta(theta) lies between two pale blue colors, and thus cannot be readily identified.

As proposed we grouped Fig. 7 in a single column and adjusted the color bar in order that the zero value can be better identified as shown in Fig. 7 of this author comment. Further we also adjusted the color bar in Fig. A1 within the Appendix of the manuscript.

Minor points of clarification, wording suggestions, and grammar / typo corrections:

1. *P1, L9: To avoid any possibility of confusion, I think 'boundary sources' should be 'boundary layer sources'; also in this line 'transport pathway' should just be 'transport'*

   done

2. *P2, L1: I think it would be better to add 'and is' between 'summer' and 'associated'*

   done

3. *P2, L9: a large variability $->$ large variability; anticyclone reaching $->$ anticyclone, which reaches*

   done

4. *P2, L13: referred $->$ referred to*

   done

5. *P3, L7-8: relation . . . influence $->$ relationship . . . influences*

   done

6. *P3, L11-12: with observations of global . . . measurements of the − > with global . . . measurements from the*

   done

7. *P3, L25: the the − > the; between 360 K − > from 360 K*

   done

8. *P3, L33: as − > us*

   done

9. *P4, L5: at top − > at the top*

   done

10. *P5, L27: having ‘Tropical AR’ in quotes and bold font gives the reader the impression that this is an important acronym that will be used again, whereas ‘tropical adjacent regions’ is always written out in full in the text. ‘Tropical AR’ seems to be used only in figure labels; in Table 1 this area is referred to as ‘TAR’. It would be better to be more consistent in the usage.*

    We removed the bold font of ‘Tropical AR’. We revised Section 3.3.3 and discussed the TAR tracer instead of SEA. Therefore, TAR tracer is more prominent and consistently used in the revised version of the manuscript.

11. *P6, L5: an added − > added*

    done

12. *P6, L22-23: associated to −> associated with; delete ‘anymore’*

    done

13. *P6, L26: Asia −> Asian*

    done

14. *P7, L6 and also L8: synoptical −> synoptic*

    done

15. *P7, L26: the 18 August −> 18 August*

    done

16. *P8, L1: and for the −> and that for the*

    done

17. *P8, L6-8: the lack of strong tracer gradients on the equatorward side of the anticyclone has been noted several times, so some references to previous work would be appropriate here.*

    We introduced the following references (e.g., Ploeger et al., 2015; Santee et al., 2017).

18. *P8, L15: low values of the tropical adjacent regions −> low fractions from the tropical adjacent regions*

    done

19. *P8, L24-25: this wording is confusing. It would be clearer to say: 'At 90E (Fig. 2c), a layer of young air masses with enhanced India/China fractions extends well above the thermal tropopause, with values as high as 20% up to 420 K.'*

    done

20. *P9, L4-5: 'in particular' is repeated twice in these lines, thus 'restricted regions, such as' would be better. In addition, this point was made previously not only in Section 1 as noted, but also in Section 2.4 (P6). It may not be necessary to provide this information three times, so the authors might consider deleting it from Section 2.4.*

    We replaced 'in particular' and removed the statement in Sect. 2.4.

21. *P9, L9: delete 'percentages of'; are marked − > is marked on the cross sections*

    done

22. *P9, L18: mode − > modes; also, I feel it would be more appropriate to say 'broadly consistent'*

    done

23. *P9, 26: it would be clearer to say 'smaller' rather than 'lower' mixing ratios (since this sentence also talks about 'below' and 'above')*

    done

24. *P10, L6-8: Restructuring this sentence would make it easier to interpret: 'At 380 K, the highest fractions of air from India/China and from the tropical adjacent regions are found in the core of the anticyclone and*

at its edge, respectively.'

done

25. *P10, L10: 'vertical upward' is redundant in this context; use one or the other, not both*

    done

26. *P10, L15: started* $->$ *starting; mode* $->$ *modes*

    done

27. *P10, L26: upward transport* $->$ *vertical transport (to avoid repeating 'upward')*

    done

28. *P10, L27: part* $->$ *parts*

    done

29. *P10, L29: western and eastern part* $->$ *western and eastern parts of the anticyclone*

    done

30. *P10, L30: 'vertical upward' - same comment as above*

    done

31. *P11, L10: mode −> modes*

    done

32. *P11, L11: to what does 'in this region' refer? The tropics, or 360 K, or ???*

    'in this region' refer to the anticyclone at 360 K.

    The pattern of $\Delta\Theta$ at 360 K within the anticyclone and in the tropics are very patchy, reflecting that the strong upward transport in this region is caused by single convective events.

33. *P11, L18: mode −> modes*

    done

34. *P11, L29: the Appendix A −> Appendix A*

    done

35. *P12, L7: boundary regions −> boundary layer regions*

    done

36. *P12, L9: winter time −> winter*

    done

37. *P12, L10: boundary emissions −> boundary layer emissions*

done

38. *P12, L17: larger as $->$ larger than; also delete ‘(Winter 07/08 pulse)’ after ‘tracer’*

    done

39. *P12, L18: winter time $->$ winter*

    done

40. *P12, L23: analysis $->$ reanalysis*

    done

41. *12, L26: tropopause which again are $->$ tropopause, which in turn are*

    done

42. *P12, L29: longitude $->$ latitude*

    done

43. *P12, L32: from Summer $->$ from the Summer*

    done

44. *P12, L34: Asia $->$ Asian*

    done

45. *P12, L31: it might be good to add 'just' here: 'a combination of just two signals', to make a stronger contrast*

    done

46. *P13, L1: winter time − > winter*

    done

47. *P13, L4: velocity − > velocities; summer time − > summer*

    done

48. *P13, L6: exists; that − > exist that*

    done

49. *P13, L11: This point was already made in Figs. 8 and 9; thus it would be better to refer back to those figures here than to point ahead to Fig. 12, which is not introduced until the following paragraph.*

    done

50. *P13, L12: boundary − > boundary layer*

    done

51. *P13, L26: highest − > largest*

    done

52. *P13, L30: boundary emission − > boundary layer emission*

done

53. *P14, L3: the the − > the*

done

54. *P15, L17: is already − > has already been*

done

55. *P16, L20: 1 K per day - 1.5 K per day − > 1-1.5 K per day (as done everywhere else in the paper)*

done

56. *P16, L22-30: these lines are a bit garbled. First, it is odd to have a 1-sentence paragraph (L22-24). Second, L30 starts with 'Further' but then repeats verbatim the sentence in L23-24. These sentences need to be merged / rearranged / rewritten. Third, the sentence in L25-26 is hard to read. It would be clearer to say: 'Thus, within the upward spiralling range above the anticyclone, young air masses from along its edge originating in the tropical adjacent regions are mixed with air masses from inside the anticyclone mainly originating in India/China.' Finally, L29: consisted − > consistent*

done

57. *P17, L2-5: It is stated that fresh emissions from the 2008 monsoon season do not contribute to the distribution within the tropical pipe at 550 K. However, emissions from that season would eventually reach 550 K, so this statement needs to be qualified in some way (for example, by*

adding 'before October 2008' or something similar). Similarly, it might be good to add 'in October 2008' after '550 K' in L5.

done

58. *P17, L8: here too I think it would be better to delete 'pathway'*

    done

59. *P17, L13-14: region air masses from the tropical adjacent regions (Southeast Asia/tropical Pacific/northern Africa/northwestern Pacific) are transported in a substantial percentage by this pathway into the tropical pipe − > region, a substantial percentage of air masses from the tropical adjacent regions (Southeast Asia/tropical Pacific/northern Africa/northwestern Pacific) is transported by this pathway into the tropical pipe.*

    done

60. *P26, Fig. 2 caption: Rather than 'first' and 'second', it may be better to refer to the tropopauses as 'primary' and 'secondary'. Also, in the last sentence, 'percentages' should be deleted, and '(cross sections)' should be added after 'white lines'.*

    done

61. *P27, Fig. 3 caption: thick black or grey lines − > thick black (maps) or grey (cross sections) lines*

    done

62. *P29, Fig. 5 caption: reversed − > back; single − > successive*

done

63. *P30, Fig. 6 caption: reversed − > back*

    done

64. *P31, Fig. 7 caption: are shown − > is shown; 1st row − > 1st panel; rows − > panels*

    done

65. *P32, Fig. 8 caption: again, 'primary' and 'secondary' may be better than 'first' and 'second'*

    done

66. *P33, Fig. 10 caption: again, 'primary' and 'secondary' may be better than 'first' and 'second'*

    done

67. *P34, Fig. 11 caption: eastern mode (80E-100E) − > eastern (80E-100E) mode*

    done

68. *P35, Fig. 12 caption: (1) this would be easier to read if '(top)' were moved to before 'The contribution' in L1 and '(bottom)' were moved to before 'The contribution' in L5. (2) 'by October 2008' should be added at the end of '550 K' in L4. (3) 'The contribution of the three time pulses' − > The contributions of the time pulses' (it is confusing to say three since only two are shown). (4) in the legend of the figure itself,*

'Residual' should be 'Residual surface' to be consistent with the text.

done

69. *P36, Fig. 13 caption: transport pathway − > transport*

    done

70. *P38, Fig. A2: In the legend, Residual − > Residual surface*

    done

References

Bergman, J. W., Jensen, E. J., Pfister, L., and Yang, Q.: Seasonal differences of vertical-transport efficiency in the tropical tropopause layer: On the interplay between tropical deep convection, large-scale vertical ascent, and horizontal circulations, J. Geophys. Res., 117, https://doi.org/10.1029/2011JD016992, 2012.

Bergman, J. W., Fierli, F., Jensen, E. J., Honomichl, S., and Pan, L. L.: Boundary layer sources for the Asian anticyclone: Regional contributions to a vertical conduit, J. Geophys. Res., 118, 2560–2575, https://doi.org/10.1002/jgrd.50142, 2013.

Chen, B., Xu, X. D., Yang, S., and Zhao, T. L.: Climatological perspectives of air transport from atmospheric boundary layer to tropopause layer over Asian monsoon regions during boreal summer inferred from Lagrangian approach, Atmos. Chem. Phys., pp. 5827–5839, https://doi.org/10.5194/acp-12-5827, 2012.

Chirkov, M., Stiller, G. P., Laeng, A., Kellmann, S., von Clarmann, T., Boone, C. D., Elkins, J. W., Engel, A., Glatthor, N., Grabowski, U., Harth, C. M., Kiefer, M., Kolonjari, F., Krummel, P. B., Linden, A., Lunder, C. R., Miller, B. R., Montzka, S. A., Mühle, J., O'Doherty, S., Orphal, J., Prinn, R. G., Toon, G., Vollmer, M. K., Walker, K. A., Weiss, R. F., Wiegele, A., and Young, D.: Global HCFC-22 measurements with MIPAS: retrieval, validation, global distribution and its evolution over 2005-2012, Atmos. Chem. Phys., 16, 3345–3368, https://doi.org/10.5194/acp-16-3345-2016, URL `www.atmos-chem-phys.net/16/3345/2016/`, 2016.

Fadnavis, S., Schultz, M. G., Semeniuk, K., Mahajan, A. S., Pozzoli, L., Sonbawne, S., Ghude, S. D., Kiefer, M., and Eckert, E.: Trends in peroxyacetyl nitrate (PAN) in the upper troposphere and lower stratosphere over southern Asia during the summer monsoon season: regional impacts, Atmos. Chem. Phys., 14, 12 725–12 743, https://doi.org/10.5194/acp-14-12725-2014, 2014.

Garny, H. and Randel, W. J.: Transport pathways from the Asian monsoon anticyclone to the stratosphere, Atmos. Chem. Phys., 16, 2703–2718, https://doi.org/10.5194/acp-16-2703-2016, 2016.

Li, D., Vogel, B., Bian, J., Müller, R., Pan, L. L., Günther, G., Bai, Z., Li, Q., Zhang, J., Fan, Q., and Vömel, H.: Impact of typhoons on the composition of the upper troposphere within the Asian summer monsoon anticyclone: the SWOP campaign in Lhasa 2013, Atmos. Chem. Phys., 17, 4657–4672, https://doi.org/10.5194/acp-17-4657-2017, URL `https://www.atmos-chem-phys.net/17/4657/2017/`, 2017.

McKenna, D. S., Konopka, P., Grooß, J.-U., Günther, G., Müller, R., Spang, R., Offermann, D., and Orsolini, Y.: A new Chemical Lagrangian Model of the Stratosphere (CLaMS): 1. Formulation of advection and mixing, J. Geophys. Res., 107, 4309, https://doi.org/10.1029/2000JD000114, 2002.

Müller, S., Hoor, P., Bozem, H., Gute, E., Vogel, B., Zahn, A., Bönisch, H., Keber, T., Krämer, M., Rolf, C., Riese, M., Schlager, H., and Engel, A.: Impact of the Asian monsoon on the extratropical lower stratosphere: trace gas observations during TACTS over Europe 2012, Atmos. Chem. Phys., 16, 10 573–10 589, https://doi.org/10.5194/acp-16-10573-2016, 2016.

Park, M., Randel, W. J., Gettleman, A., Massie, S. T., and Jiang, J. H.: Transport above the Asian summer monsoon anticyclone inferred from Aura Microwave Limb Sounder tracers, J. Geophys. Res., 112, D16309, https://doi.org/10.1029/2006JD008294, 2007.

Park, M., Randel, W. J., Emmons, L. K., and Livesey, N. J.: Transport pathways of carbon monoxide in the Asian summer monsoon diagnosed from Model of Ozone and Related Tracers (MOZART), J. Geophys. Res., 114, D08303, https://doi.org/10.1029/2008JD010621, 2009.

Ploeger, F., Konopka, P., Müller, R., Fueglistaler, S., Schmidt, T., Manners, J. C., Grooß, J.-U., Günther, G., Forster, P. M., and Riese, M.: Horizontal transport affecting trace gas seasonality in the Tropical Tropopause Layer (TTL), J. Geophys. Res., 117, D09303, https://doi.org/10.1029/2011JD017267, 2012.

Ploeger, F., Gottschling, C., Grießbach, S., Grooß, J.-U., Günther, G., Konopka, P., Müller, R., Riese, M., Stroh, F., Tao, M., Ungermann, J., Vogel, B., and von Hobe, M.: A potential vorticity-based determination of the transport barrier in the Asian summer monsoon anticyclone, Atmos. Chem. Phys., 15, 13 145–13 159, https://doi.org/doi:10.5194/acp-15-13145-2015, 2015.

Ploeger, F., Konopka, P., Walker, K., and Riese, M.: Quantifying pollution transport from the Asian monsoon anticyclone into the lower stratosphere, Atmos. Chem. Phys., 17, 7055–7066, https://doi.org/10.5194/acp-17-7055-2017, URL `https://www.atmos-chem-phys.net/17/7055/2017/`, 2017.

Randel, W. J. and Park, M.: Deep convective influence on the Asian summer monsoon anticyclone and associated tracer variability observed with Atmospheric Infrared Sounder (AIRS), J. Geophys. Res., 111, D12314, https://doi.org/10.1029/2005JD006490, 2006.

Randel, W. J., Park, M., Emmons, L., Kinnison, D., Bernath, P., Walker, K. A., Boone, C., and Pumphrey, H.: Asian Monsoon Transport of Pollution to the Stratosphere, Science, 328, 611–613, https://doi.org/10.1126/science.1182274, 2010.

Santee, M. L., Manney, G. L., Livesey, N. J., Schwartz, M. J., Neu, J. L., and Read, W. G.: A comprehensive overview of the climatological composition of the Asian summer monsoon anticyclone based on 10 years of Aura Microwave Limb Sounder measurements, Journal of

Geophysical Research: Atmospheres, 122, 5491–5514, https://doi.org/10.1002/2016JD026408, URL https://agupubs.onlinelibrary.wiley.com/doi/abs/10.1002/2016JD026408, 2017.

Schoeberl, M. R., Dessler, A. E., and Wang, T.: Simulation of stratospheric water vapor and trends using three reanalyses, Atmos. Chem. Phys., 12, 6475–6487, https://doi.org/10.5194/acp-12-6475-2012, 2012.

Tissier, A.-S. and Legras, B.: Convective sources of trajectories traversing the tropical tropopause layer, Atmos. Chem. Phys., 16, 3383–3398, https://doi.org/10.5194/acp-16-3383-2016, 2016.

Vogel, B., Günther, G., Müller, R., Grooß, J.-U., Hoor, P., Krämer, M., Müller, S., Zahn, A., and Riese, M.: Fast transport from Southeast Asia boundary layer sources to northern Europe: rapid uplift in typhoons and eastward eddy shedding of the Asian monsoon anticyclone, Atmos. Chem. Phys., 14, 12 745–12 762, https://doi.org/10.5194/acp-14-12745-2014, URL http://www.atmos-chem-phys.net/14/12745/2014/, 2014.

Vogel, B., Günther, G., Müller, R., Grooß, J.-U., and Riese, M.: Impact of different Asian source regions on the composition of the Asian monsoon anticyclone and of the extratropical lowermost stratosphere, Atmos. Chem. Phys., 15, 13 699–13 716, https://doi.org/10.5194/acp-15-13699-2015, URL http://www.atmos-chem-phys.net/15/13699/2015/, 2015.

Wright, J. S. and Fueglistaler, S.: Large differences in reanalyses of diabatic heating in the tropical upper troposphere and lower stratosphere, Atmos. Chem. Phys., 13, 9565–9576, https://doi.org/10.5194/acp-13-9565-2013, 2013.

Wright, J. S., Fu, R., Fueglistaler, S., Liu, Y. S., and Zhang, Y.: The influence of summertime convection over Southeast Asia on water vapor in the tropical stratosphere, J. Geophys. Res., 116, D12302, https://doi.org/10.1029/2010JD015416, 2011.

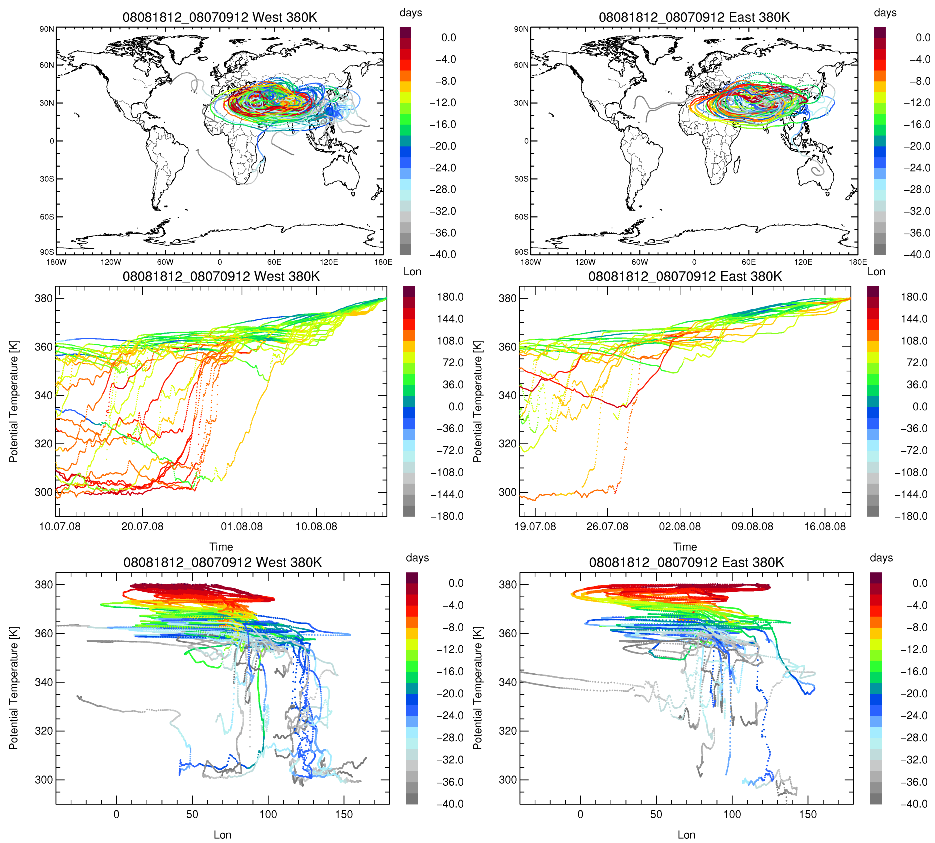

Figure 2: Different 40-day backward trajectories started at 380 K in the western (left) and eastern (right) mode of the Asian monsoon anticyclone are shown colour-coded by days back from 18 August 2008 (top). Further, potential temperature versus time (in UTC) along 40-day backward trajectories colour-coded by longitude (middle) and potential temperature versus longitude colour-coded by days back from 18 August 2008 (bottom) are shown. The trajectory positions are plotted every hour (coloured dots). Large distances between successive positions indicate rapid uplift.

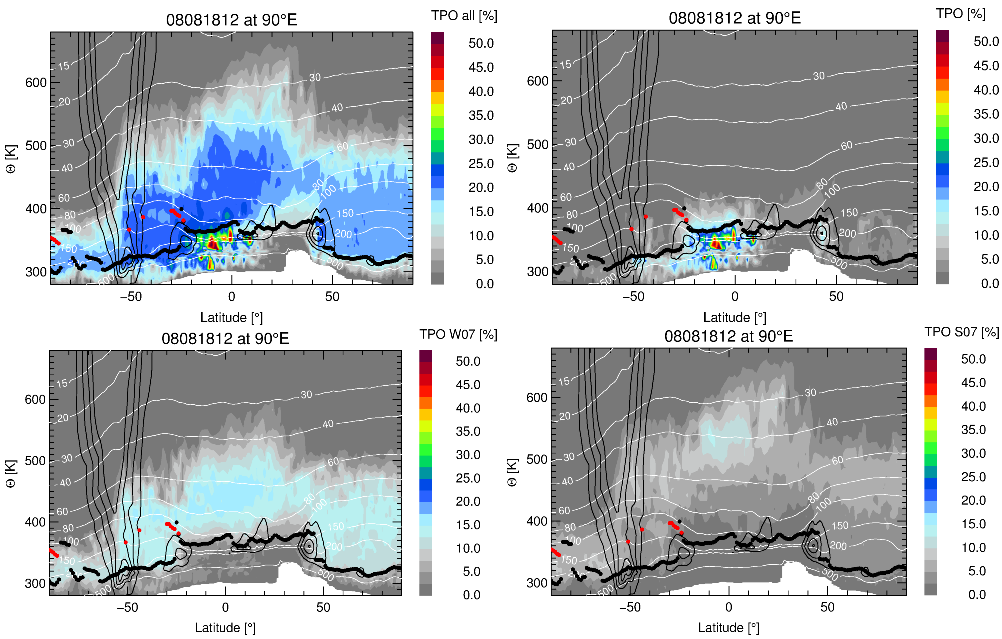

Figure 3: Latitude–theta cross sections at 90°E for the fraction of the TPO tracer for the simulation period (1 May 2007 - 18 August 2008 labeled as 'all'), for the Summer 08 (S08) pulse, for the Winter 07/08 (W07) pulse, and for the Summer 07 (S07) pulse on 18 August 2008. The thermal tropopause (primary in black dots and secondary in red dots) and horizontal winds (black lines) are shown. The corresponding levels of pressure are marked by thin white lines.

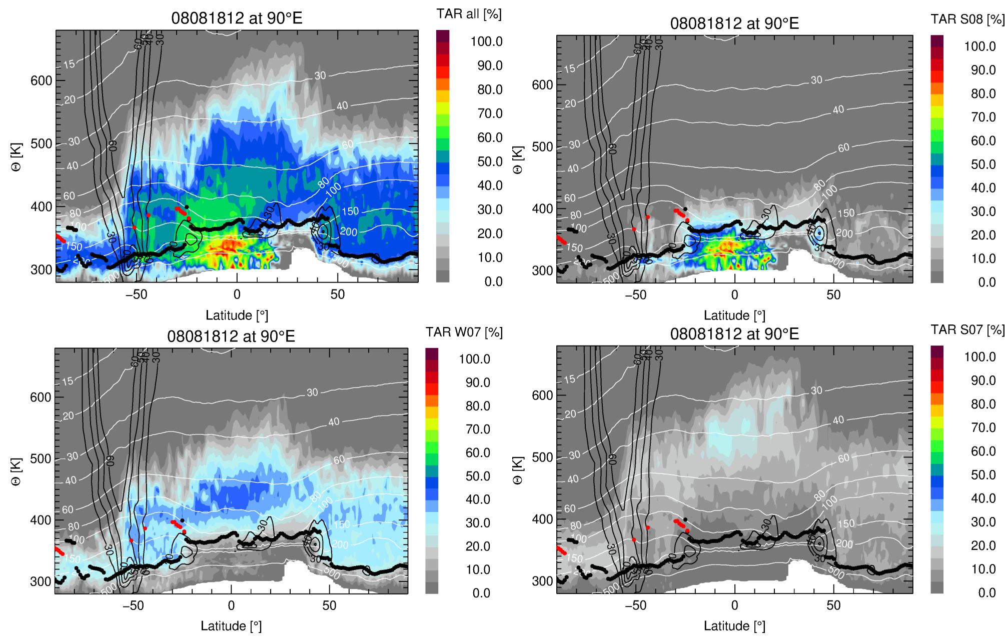

Figure 4: As Fig. 3 but for the fraction of the tracer for tropical adjacent regions (TAR)

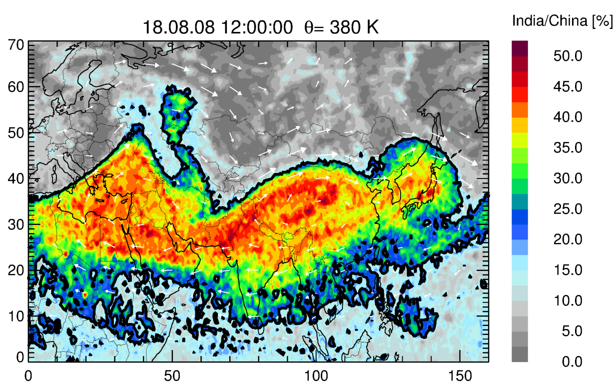

Figure 5: Horizontal distribution of the fraction of air originating in India/China at 380 K potential temperature. The contour line of 20% of the India/China tracer is shown by thick black line.

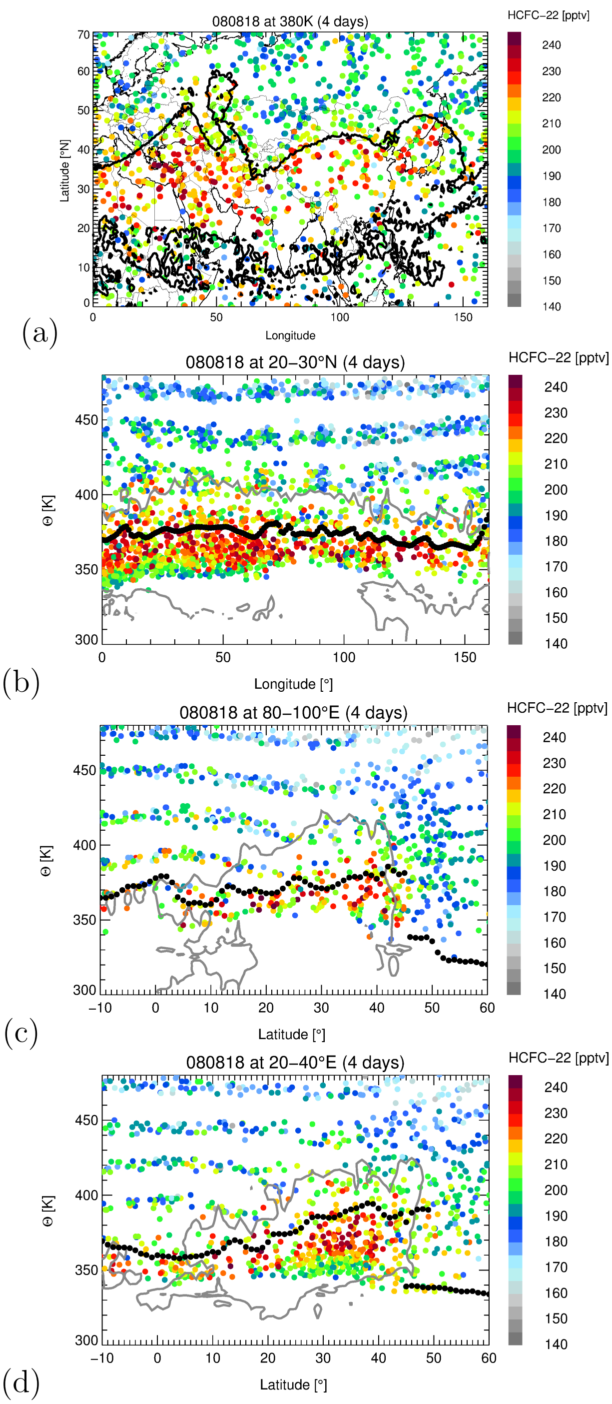

Figure 6: Horizontal distribution of MIPAS HCFC-22 measurements at 380 K potential temperature (a). The MIPAS measurements are synoptically interpolated within 4 days (for details see Sect. 2.4). Longitude–theta cross section at 25°N (b) is shown as well as latitude–theta cross sections at 90°E (eastern part of the anticyclone) (c) and at 30°E (western part of the anticyclone) (d) on 18 August 2008. The contour line of 20% of the India/China tracer is shown by thick black (maps) or grey (cross sections) lines as shown in Figs. 2 and 3. The thermal tropopause is marked by black dots.

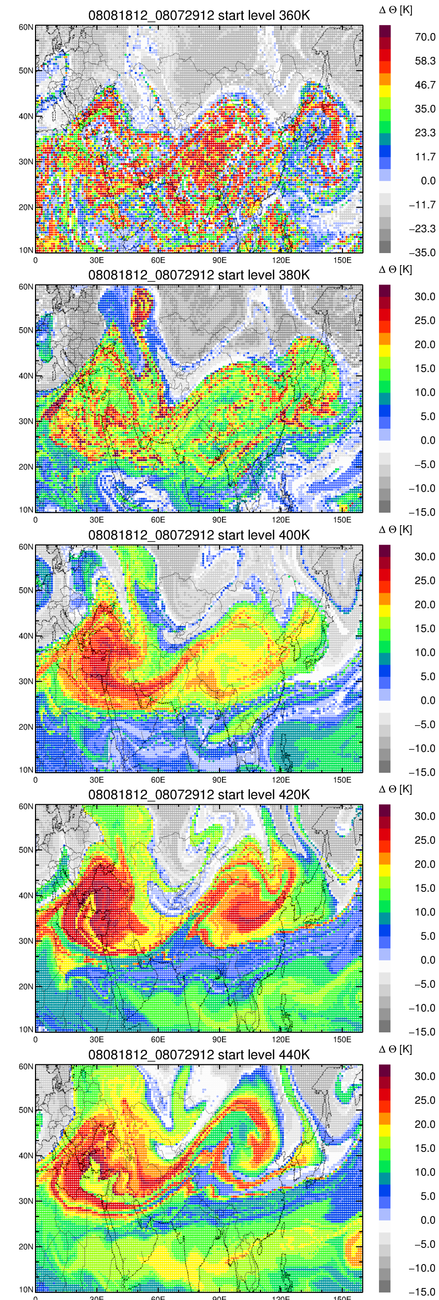

Figure 7: The change in potential temperature ($\Delta\Theta$) along 20-day backward trajectories initialised on 18 August 2008 is shown for different levels of potential temperature (360 K, 380 K, 400 K, 420 K, and 440 K). Note that the range of the colour bar in the 1st panel is much larger than in the other panels. At the lower potential temperature levels (360 K, 380 K), some 20-day backward trajectories exist that reach the model boundary layer within a time period shorter than 20 days (in cases of very strong uplift by convection). For these trajectories $\Delta\Theta$ is shown for the shorter time period.